IQ Motif and SEC7 Domain-containing Protein 3 (IQSEC3) Interacts with Gephyrin to Promote Inhibitory Synapse Formation*

Ji Won Um[‡§], **Gayoung Choii**[‡1], **Dongseok Park**[§1], **Dongwook Kim**[§], **Sangmin Jeon**[‡1], **Hyeyeon Kang**[§1], **Takuma Mori**[¶], **Theofilos Papadopoulos**[‖], **Taesun Yoo**[**], **Yeunkum Lee**[‡‡], **Eunjoon Kim**[**‡‡], **Katsuhiko Tabuchi**[¶§§], and ⬤ **Jaewon Ko**[‡2]

From the ‡Department of Biochemistry, College of Life Science and Biotechnology, Yonsei University, Seoul 120-749, Republic of Korea, the §Department of Physiology and BK21 PLUS Project for Medical Science, Yonsei University College of Medicine, Seoul 120-752, Republic of Korea, the ¶Shinshu University School of Medicine, Matsumoto 390-8621, Japan, the ‖Department of Molecular Biology, University Medicine Göttingen, Göttingen 37075, Germany, the **Department of Biological Sciences, Korea Advanced Institute of Science and Technology, Daejeon 305-701, Republic of Korea, the ‡‡Center for Synaptic Brain Dysfunctions, Institute for Basic Science, Daejeon 305-701, Republic of Korea, and §§PRESTO, Japan Science and Technology Agency, Kawaguchi 332-0012, Japan

Gephyrin is a central scaffold protein that mediates development, function, and plasticity of mammalian inhibitory synapses by interacting with various inhibitory synaptic proteins. Here, we show that IQSEC3, a guanine nucleotide exchange factor for ARF6, directly interacts with gephyrin, an interaction that is critical for the inhibitory synapse localization of IQSEC3. Overexpression of IQSEC3 increases inhibitory, but not excitatory, synapse density in a guanine nucleotide exchange factor activity-dependent manner. Conversely, knockdown of IQSEC3 decreases size of gephyrin cluster without altering gephyrin puncta density. Collectively, these data reveal that IQSEC3 acts together with gephyrin to regulate inhibitory synapse development.

Postsynaptic scaffolding proteins organize functional synapses and promote reliable synaptic transmission by ensuring the accurate accumulation of postsynaptic receptors in precise apposition to presynaptic release sites. They also provide platforms for postsynaptic receptors and regulate downstream signaling cascades to adjust the molecular composition of the postsynaptic machineries that enable postsynaptic plasticity (1, 2). The most extensively studied proteins at inhibitory synapses are arguably gephyrin and its notable binding protein, collybistin (3, 4). However, although significant progress has been made, integrated principles that would allow a comprehensive understanding of inhibitory synapse organization and development, particularly at molecular levels, remain to be established (5, 6).

Gephyrin forms a hexagonal lattice beneath the postsynaptic membrane at inhibitory synapses and anchors $GABA_A$ (γ-aminobutyric acid) and glycine receptors (4, 6–8). Gephyrin interacts with numerous other proteins whose functions at inhibitory synapses, with the exception of collybistin and neuroligin (NL)[3]-2, are largely undefined (6, 9). Collybistin is required for gephyrin clustering, and their absence in mice compromises GABAergic synaptic transmission and spatial learning (10, 11). NL-2 is an established inhibitory synaptic-adhesion molecule essential for inhibitory synaptic transmission that *trans*-synaptically interacts with presynaptic neurexins and intracellularly binds to gephyrin (12). Through its tripartite interactions with gephyrin and collybistin, NL-2 nucleates the postsynaptic apparatus, locally inducing gephyrin clustering and promoting its submembrane targeting (9).

IQSEC3 (also known as BRAG3 or SynArfGEF), together with IQSEC1 and IQSEC2, constitutes a family of brefeldin A-resistant ARF guanine nucleotide exchange factors (GEFs) (13). IQSEC family members exhibit distinct synaptic localization in mouse retina (14). IQSEC2/BRAG1 and IQSEC1/BRAG2 directly interact with PSD-95 and are involved in α-amino-3-hydroxy-5-methyl-4-isoxazolepropionic acid (AMPA)-type glutamate receptor trafficking and long term synaptic depression at excitatory synapses (15, 16). IQSEC1 is involved in signaling pathways that induce breast cancer invasion (17), and IQSEC2 mutations are associated with non-syndromic X-linked intellectual disability (18, 19). By contrast, IQSEC3 is exclusively localized to inhibitory synapses (13, 14). However, it remains to be determined whether IQSEC3 is functionally important at inhibitory synapses and, if so, how it orchestrates inhibitory synapse development and function.

[1] Fellowship awardees by the Brain Korea 21 PLUS Program.
[2] To whom correspondence should be addressed: Dept. of Biochemistry, College of Life Science and Biotechnology, Yonsei University, 134 Shinchon-dong, Seodaemun-gu, Science Research Center S421, Seoul 120-749, Republic of Korea. Tel.: 82-2-2123-5699; Fax: 82-2-362-9897; E-mail: jaewonko@yonsei.ac.kr.

[3] The abbreviations used are: NL, neuroligin; IQSEC, IQ motif and Sec7 domain; VGLUT, vesicular glutamate transporter; aa, amino acid; EGFP, enhanced GFP; DIV, days *in vitro*; GEF, guanine nucleotide exchange factor; ANOVA, analysis of variance; PSD, postsynaptic density.

Role of IQSEC3 in Inhibitory Synapse Formation

Here, we show that IQSEC3 directly binds to gephyrin to promote inhibitory synapse formation in an Arf-GEF activity-dependent manner in cultured hippocampal neurons. Gephyrin is required for inhibitory synapse localization of IQSEC3, which is critical for clustering of gephyrin in cultured hippocampal neurons. Moreover, IQSEC3 is important for maintenance of gephyrin cluster size. Our results suggest a novel molecular mechanism of inhibitory synapse formation that may link ARF activity to the IQSEC3-gephyrin complex and further imply that IQSEC3 is critical for mediating neuronal inhibition, possibly hinting at its crucial roles in organizing inhibitory neural circuit properties.

Experimental Procedures

Yeast Two-hybrid Screens

Yeast two-hybrid screening was performed as described previously (20) using the PBN204 yeast strain harboring *URA3*, *ADE2,* and β-gal as reporter genes. Full-length gephyrin (aa 2–736) was subcloned into pGBKT (Gal4 fusion vector; Clontech) and used to screen ~1.0×10^6 clones from a human brain cDNA library (Clontech) constructed in pACT2 (Gal4 activation domain vector; Clontech). All of the prey clones were verified by nucleotide sequencing.

Construction of Expression Vectors

IQSEC3—Expression plasmids for fragments of rat IQSEC3 (GenBank[TM] accession number, NM_207617) were prepared by amplifying the corresponding region of the gene by PCR and subcloning into the pCAGGS-FLAG vector at EcoRI/EcoRV sites. Fragments corresponding to the following amino acid (aa) regions were prepared: 1–350; 1–315; 336–655; 1–995; 336–995; 336–1194; 636–1194; 1–100; 101–200; 996–1194; 996–1095; and 1–1190. cDNA encoding full-length rat IQSEC3 (aa 1–1194) was PCR-amplified and subcloned into the pcDNA3.1 Myc vector (Invitrogen) at EcoRI/EcoRV sites. The Arf-GEF-inactive mutant E749A was generated by QuikChange site-directed mutagenesis (Stratagene) using pcDNA3.1 Myc-IQSEC3 as a template. The shRNA lentiviral expression vector against *Iqsec3* was constructed by annealing, phosphorylating, and cloning oligonucleotides targeting rat *Iqsec3* (5′-GAG CTG GTG GTA GGC TCT ATG AAA-3′) into the XhoI and XbaI sites of a single KD vector (L-309; see Ref. 21 for a schematic diagram of L-309) immediately downstream of the human H1 promoter. For the IQSEC3 rescue vector, three nucleotides (underlined) in the GAGCT<u>A</u>GTGGT<u>C</u>GGCTCTA<u>C</u>GAAA sequence of pcDNA3.1 Myc-IQSEC3 or pCAGGS-FLAG-IQSEC3 were mutated to render them shRNA-resistant (see Fig. 9*H*). IQSEC3 cDNA fragments corresponding to amino acids 1–185 and 311–645 were cloned into the BamHI and EcoRI sites of the pGEX4T-1 vector (GE Healthcare).

Gephyrin—Expression plasmids for fragments of rat gephyrin (GenBank[TM] accession number, NM_022865) were prepared by PCR-amplifying and subcloning the corresponding region of the gene into the pcDNA3.1 Myc vector (Invitrogen) at HindIII/XhoI sites. Fragments corresponding to the following aa regions were prepared: 1–185 (gephyrin-G); aa 166–322 (gephyrin-C); and aa 303–736 (gephyrin-E). The shRNA lentiviral expression vector against gephyrin was constructed by annealing, phosphorylating, and cloning oligonucleotides targeting rat gephyrin (5′-ACA TCA GAC CCA TCG GCC ACG ACA TTA-3′) into the XhoI and XbaI sites of the L-309 vector. A cDNA fragment of gephyrin (corresponding to aa 1–185) was cloned into the BamHI and EcoRI sites of the pRSETA vector (Thermo Fisher Scientific).

Previously Published Reagents—The following constructs were as described previously: *Myc-gephyrin* (22); *pCAGGS-FLAG-IQSEC1*, *pCAGGS-FLAG-IQSEC2*, and *pCAGGS-FLAG-IQSEC3* (a gift from Hiroyuki Sakagami) (13).

Antibodies

Fusion proteins of glutathione *S*-transferase (GST) and rat IQSEC3 (aa 1–185) were produced in BL21 *Escherichia coli* and purified on a glutathione-Sepharose column (GE Healthcare). Following immunization of rabbits with this immunogen, the IQSEC3-specific antibody JK079 was affinity-purified using a Sulfolink column (Pierce) on which the same GST-fused IQSEC3 protein was immobilized. The following commercially available antibodies were used: mouse monoclonal anti-HA (clone HA-7; Covance); mouse monoclonal anti-FLAG (clone M1; Sigma); mouse monoclonal anti-Myc (clone 9E10; Santa Cruz Biotechnology); goat polyclonal anti-EGFP (Rockland); mouse monoclonal anti-NL-1 (clone N97A/31; NeuroMab); rabbit polyclonal anti-NL-2 (Synaptic Systems); guinea pig polyclonal anti-VGLUT1 (Millipore); mouse monoclonal anti-GAD67 (clone 1G10.2; Millipore); mouse monoclonal anti-PSD-95 (clone K28/43; Thermo Scientific); mouse monoclonal anti-α-tubulin (clone DM1A; Sigma); mouse monoclonal anti-gephyrin (clone 3B11; Synaptic Systems); mouse monoclonal anti-gephyrin (clone mAb7a; Synaptic Systems); rabbit polyclonal anti-collybistin (Synaptic Systems); and mouse monoclonal anti-GABARγ2 (clone 331A12; Synaptic Systems). The following antibodies were previously described: anti-S-SCAM (1146) (23) and anti-IgSF9b (1913) (24).

Co-immunoprecipitation Assays

Rat brain homogenates from P42 rats were incubated with anti-IQSEC3 antibody (JK079) overnight at 4 °C, after which 30 μl of a 1:1 suspension of protein A-Sepharose (Incospharm Corp.) was added, and the mixture was incubated for 2 h at 4 °C with gentle rotation. In detail, rat brains (2 g) were homogenized in 10 ml of ice-cold homogenization buffer consisting of 320 mM sucrose, 5 mM HEPES-NaOH (pH 7.5), 1 mM EDTA, 0.2 mM PMSF, 1 μg/ml aprotinin, 1 μg/ml leupeptin, 1 μg/ml pepstatin, and 1 mM Na_3VO_4. The homogenized tissue was centrifuged at 2000 × *g* for 15 min, and then the supernatant was centrifuged at 100,000 × *g* for 1 h. The pellets were homogenized in buffer consisting of 20 mM HEPES-NaOH (pH 7.5), 0.15 M NaCl, 2 mM $CaCl_2$, 2 mM $MgCl_2$, 0.2 mM PMSF, 1 μg/ml aprotinin, 1 μg/ml leupeptin, 1 μg/ml pepstatin, and 1 mM Na_3VO_4. Triton X-100 was added to a final concentration of 1% (w/v) and dissolved with constant stirring at 4 °C for 1 h. Supernatants obtained after centrifugation at 100,000 × *g* for 1 h were used for co-immunoprecipitation assays. The beads were pelleted and washed three times with lysis buffer (20 mM HEPES-NaOH (pH 7.5), 0.15 M NaCl, 2 mM $CaCl_2$, 2 mM $MgCl_2$, 1% Triton X-100, 0.2 mM PMSF, 1 μg/ml aprotinin, 1 μg/ml leu-
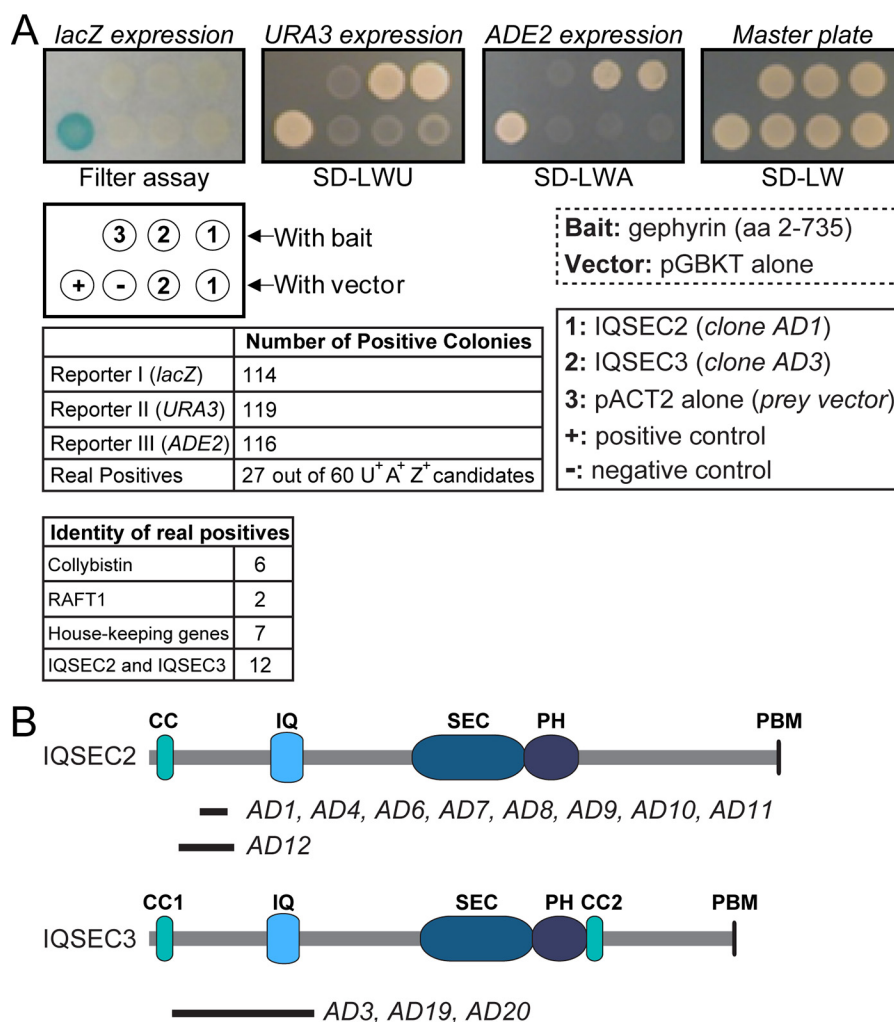
FIGURE 1. **Yeast two-hybrid screen identifies IQSEC3 as a gephyrin-binding protein.** *A*, overview of the yeast two-hybrid screen of a human brain cDNA library using gephyrin full-length cDNA (aa 2–753) cloned into the pGBKT vector. *SD-LWU*, selective medium lacking leucine, tryptophan, and uracil; *SD-LWA*, selective medium lacking leucine, tryptophan, and alanine; *SD-LW*, selective medium lacking leucine and tryptophan. *B*, human brain cDNA clones isolated from the yeast two-hybrid screen (*A*) are shown aligned below a schematic of IQSEC2 and IQSEC3 protein (drawn to scale). The prey clones are labeled *AD*. *CC1*, coiled-coil motif 1; *IQ*, calcium/calmodulin-binding IQ motif; *SEC*, Sec7 domain; *PH*, pleckstrin homology domain; *CC2*, coiled-coil motif 2; *PBM*, PDZ-binding motif.

peptin, 1 μg/ml pepstatin, and 1 mM Na$_3$VO$_4$). Immune complexes were then resolved by SDS-PAGE and immunoblotted with anti-gephyrin, anti-NL-1, anti-NL-2, anti-S-SCAM, anti-collybistin, or anti-IQSEC3 antibodies. For Figs. 2*A* and 3, *B* and *D*, human embryonic kidney 293T (HEK293T) cells were maintained in Dulbecco's modified Eagle's medium (DMEM) containing 10% fetal bovine serum (FBS) and 100 units/ml penicillin/streptomycin. HEK293T cells were then transfected with the indicated combination of plasmids. After 48 h, the transfected HEK293T cells were rinsed with ice-cold phosphate-buffered saline (PBS) and solubilized in lysis buffer (20 mM Tris (pH 7.4), 1.0% Triton X-100, 0.1% SDS, 150 mM NaCl, 10% glycerol, 0.2 mM PMSF, 1 μg/ml aprotinin, 1 μg/ml leupeptin, 1 μg/ml pepstatin, and 1 mM Na$_3$VO$_4$). After centrifugation at 20,000 $\times$ *g*, the supernatants were incubated with 1 μg of the appropriate antibody overnight at 4 °C. Thereafter, 30 μl of a 1:1 suspension of protein A-Sepharose (Incospharm Corp.) was added, and the mixture was incubated for 2 h at 4 °C with gentle rotation. Immune complexes were then resolved by SDS-PAGE and immunoblotted with the indicated antibodies. Co-immu-

noprecipitation experiments were repeated at least three times, and quantified results are expressed as the amount of protein co-precipitated relative to input amount. Representative immunoblot images are presented in the indicated figures.

Quantitative Reverse Transcription PCR

Cultured rat cortical neurons were infected with recombinant lentiviruses at DIV3 and harvested at DIV10 for quantitative real time PCR using SYBR Green quantitative PCR master mix (Takara). Total RNA was extracted from rat cortical neurons using the TRIzol reagent (Invitrogen) according to the manufacturer's protocol. Briefly, one well of a 12-well plate of cultured neurons was harvested and incubated with 500 μl of TRIzol reagent at room temperature for 5 min. After phenol/chloroform separation, RNA in the upper aqueous phase was precipitated. cDNA was synthesized from 500 ng of RNA by reverse transcription using a ReverTra Ace-α-kit (Toyobo). Quantitative PCR was performed with 1 μl of cDNA using CFX96 Touch real time PCR (Bio-Rad). The ubiquitously expressed glyceraldehyde-3-
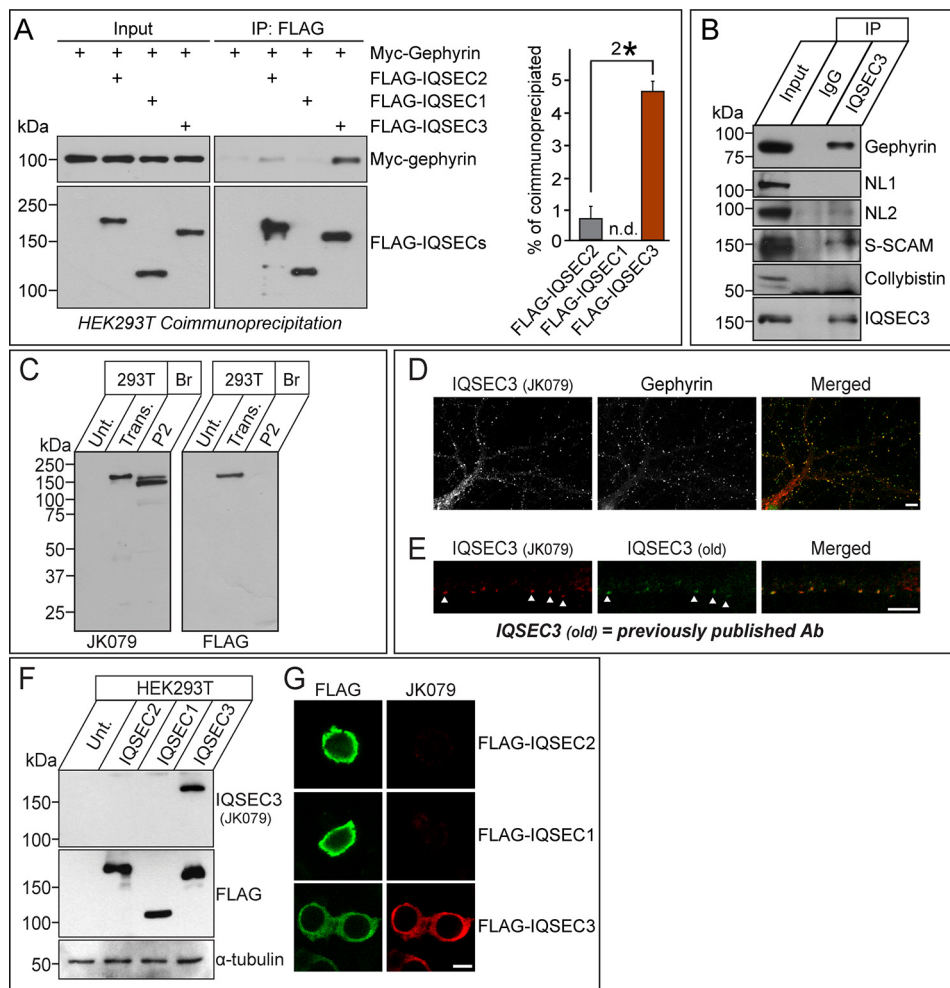
FIGURE 2. **Interaction of IQSEC3 with gephyrin in HEK293T cells, formation of an IQSEC3-gephyrin complex in rat brains, and characterization of IQSEC3 antibodies.** *A*, co-immunoprecipitation (*IP*) experiment demonstrating that IQSEC2 and IQSEC3, but not IQSEC1, interact with gephyrin. HEK293T cells were transfected with FLAG-tagged IQSEC1 (*FLAG-IQSEC1*), FLAG-tagged IQSEC2 (*FLAG-IQSEC2*), or FLAG-tagged IQSEC3 (*FLAG-IQSEC3*) alone or together with Myc-tagged gephyrin (*Myc-Gephyrin*), and co-immunoprecipitation of IQSECs with gephyrin was assayed. A representative immunoblot visualized by ECL (*left*) and quantitative *bar graphs* (*right*) analyzing co-immunoprecipitation efficiency are shown. Note that maximum co-immunoprecipitation efficiency could not be achieved. Input, 5%. *n.d.*, not determined. *B*, co-immunoprecipitation experiment in rat brains demonstrating that IQSEC3 forms complexes with gephyrin, NL-2, and S-SCAM but not with NL-1 or collybistin. Crude synaptosomal fractions of adult mouse brains were immunoprecipitated with anti-IQSEC3 antibody (JK079) and immunoblotted with the indicated antibodies. Equal amounts of rabbit IgG (IgG) were used as a negative control. Input, 5%. *C*, biochemical characterization of the anti-IQSEC3 antibody used in this study. Immunoblot analyses of the anti-IQSEC3 antibody, JK079, using rat brain crude synaptosomes (*P2*) and lysates from HEK293T cells transfected with a FLAG-tagged IQSEC3 expression vector (*Trans.*). The expression of FLAG-tagged IQSEC3 was confirmed by immunoblotting with an anti-FLAG antibody. *Br.*, brain; *P2*, crude synaptosomes; *Unt.*, untransfected HEK293T cell lysates. *D*, co-localization of IQSEC3 puncta with gephyrin puncta in rat cultured hippocampal neurons. Cultured neurons at DIV14 were immunostained with anti-IQSEC3 (JK079; *red*) and anti-gephyrin antibodies (*green*) and detected with Cy3- or FITC-conjugated secondary antibodies. *Scale bar,* 10 μm (applies to all images). *E*, validation of the in-house IQSEC3 antibody (JK079; *red*) by immunocytochemistry using DIV14 rat primary hippocampal cultured neurons. JK079-immunoreactive puncta co-localize with those obtained using previously published antibodies (old). *Scale bar,* 10 μm (applies to all images). *F* and *G*, cross-reactivity of the anti-IQSEC3 antibody. HEK293T cells, untransfected or transfected with the indicated IQSEC expression vectors, were immunoblotted or immunostained with anti-IQSEC3 (JK079) and anti-FLAG antibodies. JK079 is specific for IQSEC3. An anti-α-tubulin antibody was used for normalization. *Scale bar,* 10 μm (applies to all images).

phosphate dehydrogenase (GAPDH) was used as an endogenous control. The sequences of the primer pairs used are as follows: *IQSEC1*, 5'-TGC CAT CAT CCT CCT CAA-3' (forward) and 5'-CGA TGA GCT TCT CAA CCT TCT-3' (reverse); *IQSEC2*, 5'-TGC CAT CAT CCT CCT CAA-3' (forward) and 5'-CAC CAT TGT CAA CTC CTC TC-3' (reverse); and *IQSEC3*, 5'-GGA GCA GAT TCG GAT AGA ATG G-3' (forward) and 5'-GGG TGA TCC TTG CTT TGA CT-3' (reverse).

Neuron Culture, Transfections, Imaging, and Quantitation

Cultured hippocampal neurons were prepared from E18 rat brains, as described previously (25), cultured on coverslips coated with poly-L-lysine, and grown in Neurobasal medium supplemented with B-27 (Invitrogen), 0.5% fetal bovine serum, 0.5 mM Glutamax (Invitrogen), and sodium pyruvate (Invitrogen). For overexpression of IQSEC3 in cultured neurons, hippocampal neurons were transfected with pCAGG-FLAG-IQSEC3 or its various derivatives, as indicated in the individual figures, or with EGFP (Control) using a CalPhos kit (Clontech) at DIV10 and immunostained at DIV14. For KD of IQSEC3 in cultured neurons, hippocampal neurons were transfected with L-309 alone (control), L-309 sh-IQSEC3 (B3; IQSEC3-KD), or co-transfected with IQSEC3-KD and shRNA-resistant Myc-IQSEC3 using a CalPhos kit (Clontech) at DIV8 and immunostained at DIV14. For immunocytochemistry, cultured neurons
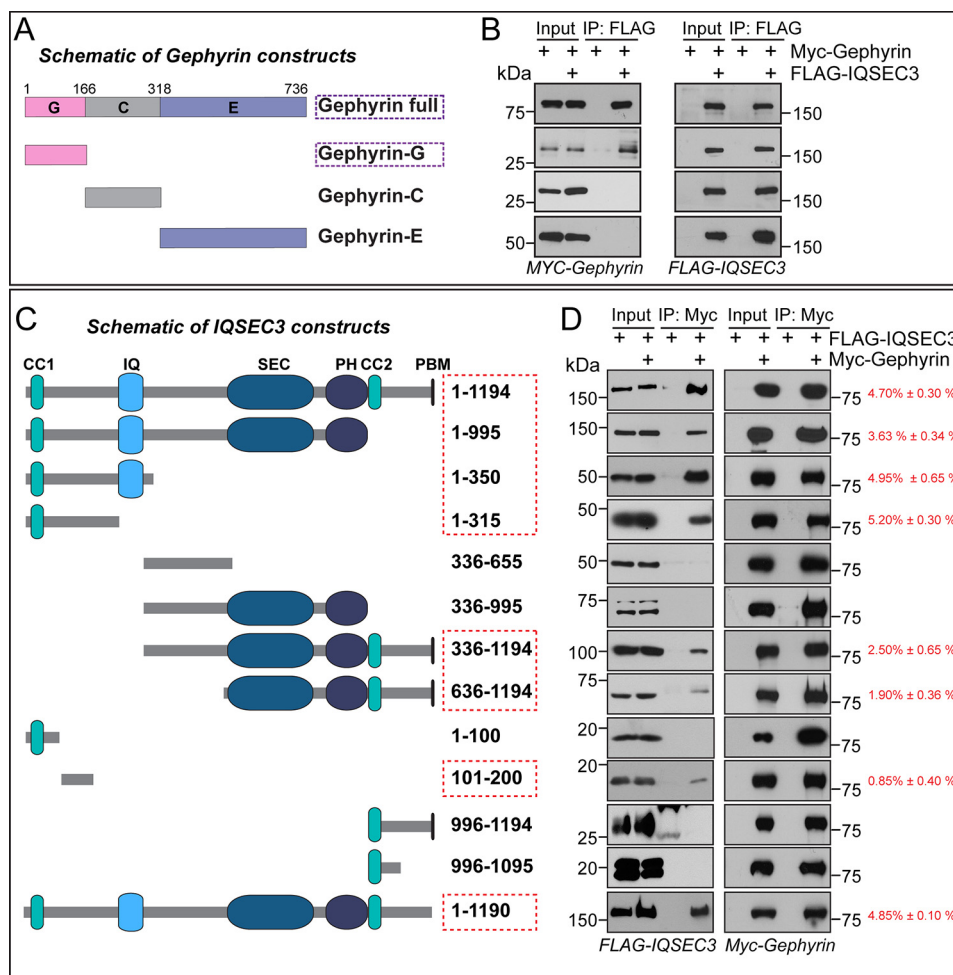
FIGURE 3. **Determination of minimal binding regions of gephyrin and IQSEC3.** *A,* schematic diagrams of a series of gephyrin deletion constructs. *G,* G-domain; *C,* C-domain; *E,* E-domain. *B,* co-immunoprecipitation (*IP*) experiment showing that the G-domain of gephyrin is sufficient for interaction with IQSEC3. HEK293T cells were transfected with Myc-tagged gephyrin (*MYC-Gephyrin*) alone or together with FLAG-tagged IQSEC3 (*FLAG-IQSEC3*), and co-immunoprecipitation of IQSEC3 with gephyrin constructs was assayed. Input, 5%. *C,* schematic diagrams of a series of IQSEC3 deletion constructs. *CC1,* coiled-coil motif 1; *IQ,* calcium/calmodulin-binding IQ motif; *SEC,* Sec7 domain; *PH,* pleckstrin homology domain; *CC2,* coiled-coil motif 2; and *PBM,* PDZ-binding motif. *D,* co-immunoprecipitation experiment showing that two regions (aa 101–200 and 636–1195) of IQSEC3 are required for interaction with gephyrin. HEK293T cells were transfected with Myc-gephyrin alone or together with FLAG-IQSEC3 constructs, and co-immunoprecipitation of IQSEC3 deletion variants with gephyrin construct was assayed and quantified as the percentage of co-immunoprecipitation efficiency (*red*). Input, 5%.

were fixed with 4% paraformaldehyde, 4% sucrose, permeabilized with 0.2% Triton X-100 in PBS, immunostained with primary antibodies as indicated, and detected with Cy3-conjugated and fluorescein isothiocyanate (FITC)-conjugated secondary antibodies (Jackson ImmunoResearch). Images were acquired using a confocal microscope (LSM710, Carl Zeiss) with a ×63 objective lens; all image setting were kept constant. Z-stacked images were converted to maximal projection and analyzed to obtain the size, intensity, and density of puncta immunoreactivities derived from marker proteins. Quantification was performed in a blind manner using MetaMorph software (Molecular Devices).

Statistics

All data are expressed as means ± S.E. All experiments were repeated using at least three independent cultures, and data were statistically evaluated using Student's *t* test or ANOVA with Tukey's test.
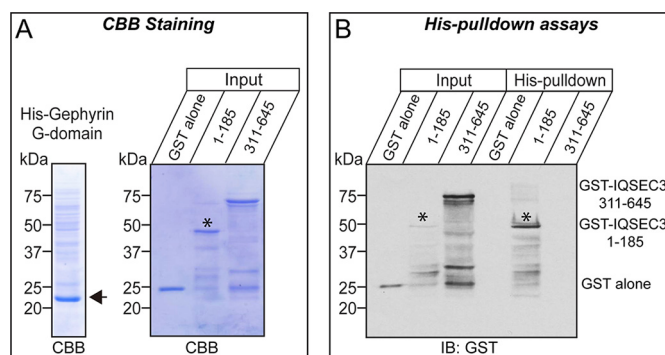

FIGURE 4. **Direct interaction of gephyrin with IQSEC3.** *A,* purified recombinant His-tagged gephyrin or GST-tagged IQSEC3 proteins produced in *E. coli* are analyzed by SDS-PAGE and Coomassie Brilliant Blue (*CBB*) staining. An *asterisk* indicates the position of purified GST-IQSEC3 aa 1–185. *B,* direct interaction of IQSEC3 with gephyrin *in vitro*. GST-IQSEC3 (aa 1–185 or aa 331–645) or GST alone was incubated with His$_6$-gephyrin. The precipitates were analyzed by immunoblotting (*IB*) with GST antibodies. *Asterisks* denote the position of purified GST-IQSEC3 (aa 1–185) bands. Input, 5%.
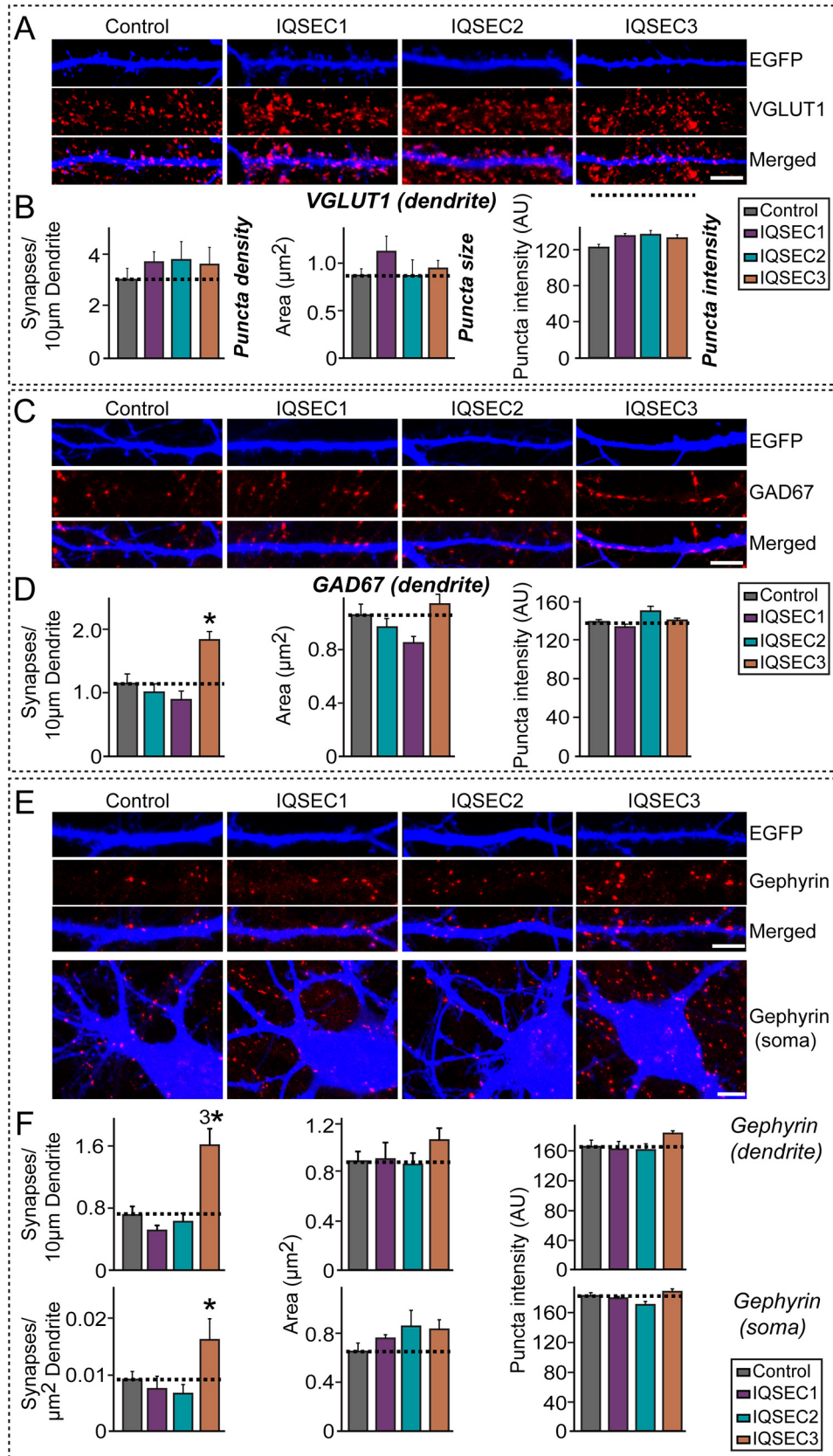
Results

Identification of IQSEC3 as a Novel Gephyrin-interacting Protein—To identify additional gephyrin-binding proteins, we screened a human brain DNA library by yeast two-hybrid assay using full-length gephyrin (aa 2–735) as bait. Of $\sim 1 \times 10^6$ yeast colonies, 60 positive clones were selected using three independent reporters, 27 of which were found to be genuine positives (Fig. 1*A*). Among these clones were eight encoded previously known gephyrin-binding proteins (six for collybistins and two for RAFT-1) (Fig. 1*A*). Intriguingly, nine encoded a partial cDNA for IQSEC2/BRAG1, and three encoded a cDNA fragment for IQSEC3/BRAG3 covering an N-terminal region between a CC1 (coiled-coil 1) domain and an IQ motif (Fig. 1*B*).

Co-immunoprecipitation assays in HEK293T cells expressing FLAG-tagged IQSEC1, IQSEC2, or IQSEC3 and Myc-tagged gephyrin confirmed these results, showing that IQSEC2 and IQSEC3, but not IQSEC1, co-immunoprecipitated with gephyrin (Fig. 2*A*). Quantitative analyses revealed that gephyrin more strongly interacted ($\sim$4.3-fold) with IQSEC3 than with IQSEC2 (Fig. 2*A*). Thus, despite structural similarities among IQSEC family proteins, only IQSEC2 and IQSEC3 were found to bind gephyrin. For this study, we focused on IQSEC3 because it is exclusively localized to inhibitory postsynaptic specializations in brains (13, 14). Next, we found that IQSEC3 immunoprecipitated from crude synaptosome lysates of adult rat brains with IQSEC3 antibodies (JK079; see below) co-immunoprecipitated significant amounts of gephyrin as well as NL-2 and S-SCAM, but not NL-1 or collybistin (Fig. 2*B*). Immunocytochemistry analyses performed using an IQSEC3-specific antibody (JK079) generated in our laboratory (Fig. 2, *C–F*) revealed strong co-localization of IQSEC3 and gephyrin in mature hippocampal neurons ($63 \pm 4\%$ of gephyrin puncta were positive for IQSEC3) (Fig. 2, *D* and *E*). This antibody specifically recognized a single band in HEK293T cells expressing IQSEC3 and two distinct bands of $\sim$150–170 kDa in brain crude synaptosomes (Fig. 2*C*). Taken together, these results indicate that IQSEC3 shares similar biochemical and expression properties and forms specific complexes with gephyrin in rat brains, in accordance with the previous reports of strong co-localization of IQSEC3 with gephyrin in brains and cultured neurons (13, 14).

Minimal Binding Domains of Gephyrin-IQSEC3 Interaction—To determine the minimal regions responsible for the interaction, we generated a series of gephyrin and IQSEC3 deletion variants and performed co-immunoprecipitation assays in HEK293T cells. We found that the G-domain, but not other
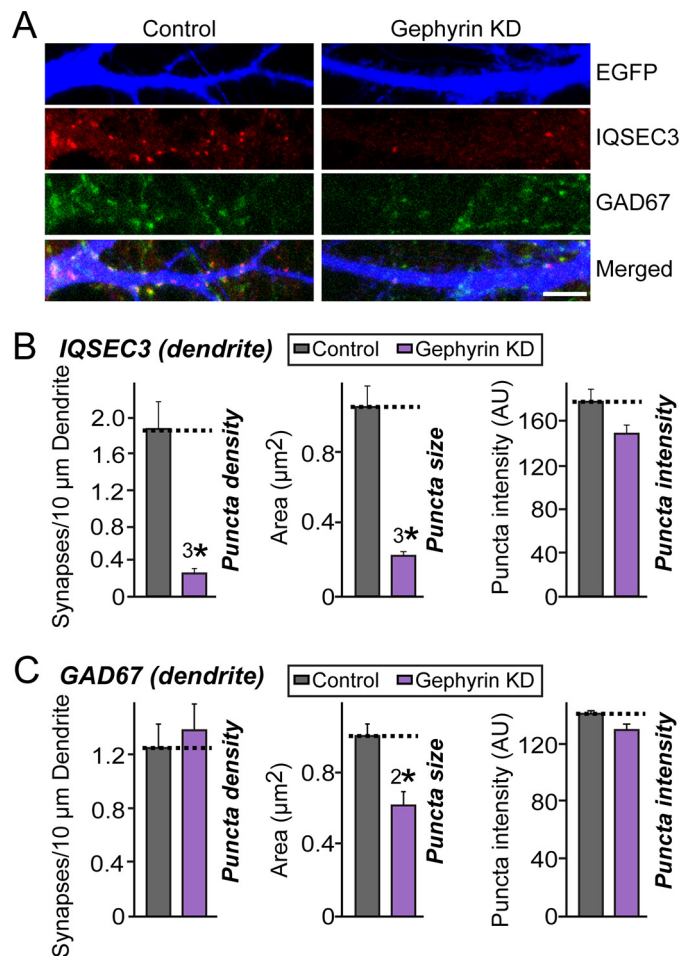

FIGURE 6. **Gephyrin is required for inhibitory synaptic localization of IQSEC3 in cultured neurons.** *A,* representative images of cultured hippocampal neurons transfected at DIV8 with lentiviral constructs expressing EGFP alone (*Control*) or co-expressing EGFP with shRNAs against gephyrin (*Gephyrin KD*). Neurons were analyzed by triple immunofluorescence labeling for IQSEC3 (*red*), GAD67 (*green*), and EGFP (*blue*) at DIV14. *Scale bar,* 10 μm (applies to all images). *B,* summary graphs of the effects of gephyrin KD in neurons on density (*left*), size (*middle*), and intensity (*right*) of IQSEC3 puncta. At least five to eight dendrites per transfected neuron were analyzed and group-averaged. Data are presented as means $\pm$ S.E. ([3]*, $p < 0.001$; Student's *t* test). *C,* same as *B,* except that density (*left*), size (*middle*), and intensity (*right*) of GAD67 puncta were quantified. Data are presented as means $\pm$ S.E. ([2]*, $p < 0.01$; Student's *t* test). *AU,* arbitrary units.

domains, of gephyrin interacted with IQSEC3 (Fig. 3, *A* and *B*). Intriguingly, the minimal gephyrin-binding region in IQSEC3 was mapped to two parts as follows: an N-terminal region (aa 101–200) and a C-terminal region (aa 636–1194). Both bound to gephyrin, although their individual binding strengths were

FIGURE 5. **IQSEC3 promotes inhibitory synapse formation in cultured hippocampal neurons.** *A,* representative images of cultured hippocampal neurons transfected at DIV10 with EGFP alone (*Control*) or together with IQSEC3 constructs (*IQSEC1, IQSEC2,* or *IQSEC3*). Neurons were analyzed by double immunofluorescence labeling for VGLUT1 (*red*) and EGFP (*blue*; pseudo-colored) at DIV14. *Scale bar,* 10 μm (applies to all images). *B,* summary graphs of the effects of IQSEC overexpression in neurons on excitatory synapse density (*left*), excitatory synapse size (*middle*), and excitatory synapse strength (*right*), as measured using VGLUT1 as an excitatory presynaptic marker. At least five to eight dendrites per transfected neuron were analyzed and group-averaged. Data are presented as means $\pm$ S.E. *C,* same as *A,* except that the transfected neurons were analyzed by double immunofluorescence labeling for GAD67 (*red*) and EGFP (*blue*) at DIV14. *Scale bar,* 10 μm (applies to all images). *D,* summary graphs of the effects of IQSEC overexpression in neurons on GAD67-positive inhibitory presynapse density (*left*), inhibitory presynapse size (*middle*), and inhibitory presynapse strength (*right*). Data are presented as means $\pm$ S.E. (*, $p < 0.05$; ANOVA with Tukey's test). *E,* same as *A,* except that dendrites and soma of transfected neurons were analyzed by double immunofluorescence labeling for gephyrin (*red*) and EGFP (*blue*) at DIV14. *Scale bar,* 10 μm (applies to all images). *F,* summary graphs of the effects of IQSEC overexpression in neurons on gephyrin-positive inhibitory postsynapse density (*left*), inhibitory postsynapse size (*middle*), and inhibitory postsynapse strength (*right*). At least five to eight dendrites or one soma per transfected neuron was analyzed and group-averaged. Data are presented as means $\pm$ S.E. (*, $p < 0.05$; [3]*, $p < 0.001$; ANOVA with Tukey's test). More than 800 gephyrin puncta were quantified in an individual image. *AU,* arbitrary units.
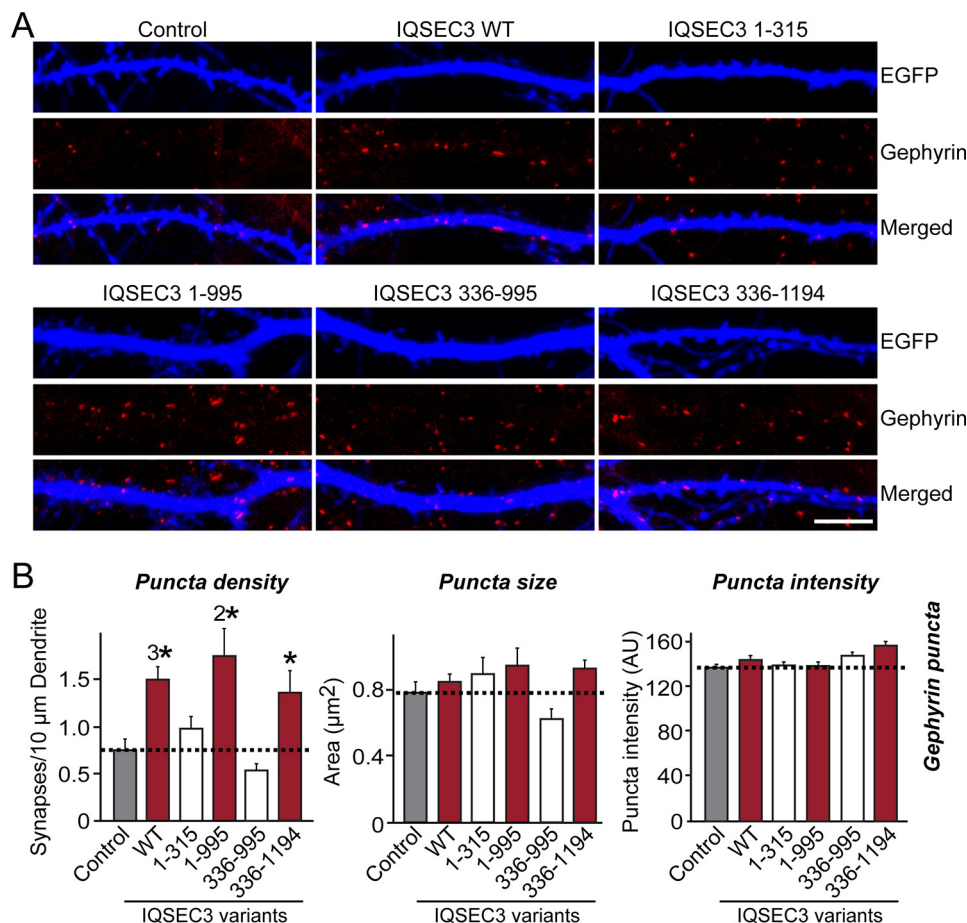
FIGURE 7. **Gephyrin-IQSEC3 interaction is required for IQSEC3-mediated promotion of inhibitory synapse formation.** *A,* representative images of cultured hippocampal neurons transfected at DIV10 with EGFP alone (*Control*) or together with the indicated IQSEC3 deletion constructs. Neurons were analyzed by double immunofluorescence labeling for gephyrin (*red*) and EGFP (*blue*) at DIV14. *Scale bar,* 10 μm (applies to all images). For detailed information regarding IQSEC3 deletion constructs, please see Fig. 3. *B,* summary graphs showing the effects of overexpressing IQSEC3 deletion constructs in neurons on gephyrin puncta density (*left*), gephyrin puncta size (*middle*), and gephyrin puncta intensity (*right*), measured using gephyrin as an inhibitory postsynaptic marker. At least five to eight dendrites per transfected neuron were analyzed and group-averaged. Data are presented as means ± S.E. (*, $p < 0.05$; [2]*, $p < 0.01$; [3]*, $p < 0.001$ *versus* control group; ANOVA Tukey's test). More than 500 gephyrin puncta were quantified in an individual image. *AU,* arbitrary units.

weaker than that of full-length IQSEC3 (aa 1–1194) (Fig. 3, *C* and *D*). In addition, His-gephyrin G-domain brought down GST-fused IQSEC3 aa 1–185, but not GST-IQSEC3 aa 311–645, suggesting that the G-domain of gephyrin directly binds to IQSEC3 (Fig. 4). Quantitative analyses showed that the N-terminal binding site had a stronger binding affinity for gephyrin than the C-terminal binding site (Fig. 3, *C* and *D*). These results suggest that two parts of the IQSEC3 molecule interact with the G-domain of gephyrin.

Overexpression of IQSEC3 Promotes Inhibitory Synapse Formation through Its Arf-GEF Activity—Next, to determine whether IQSEC3 affects inhibitory synapse development, we co-transfected cultured hippocampal neurons at DIV10 with expression vectors encoding EGFP alone (control) or EGFP with FLAG-tagged IQSEC1, IQSEC2, or IQSEC3 and immunostained transfected neurons for the excitatory synaptic marker VGLUT1 (vesicular glutamate transporter 1), the inhibitory presynaptic marker GAD67 (glutamic acid decarboxylase 67 kDa), or the inhibitory postsynaptic marker gephyrin at DIV14. Because certain inhibitory synaptic proteins preferentially act in specific subcellular domains of specific neuron types (9, 26), we analyzed GAD67- and gephyrin-positive puncta in both

dendrites and soma. Overexpression of IQSEC3 did not alter excitatory synapse density, labeled as VGLUT1-positive puncta (Fig. 5, *A* and *B*). However, overexpression of IQSEC3, but not IQSEC1 or IQSEC2, caused an increase in GAD67-positive or gephyrin-positive puncta density in both dendritic and perisomatic regions (Fig. 5, *C–F*, data not shown), suggesting that IQSEC3 specifically fosters inhibitory synapse formation in both subcellular compartments. Consistent with this, overexpression of IQSEC3 led to an increase in the number of GABA$_A$γ2 puncta in dendrites or soma of the transfected neurons (data not shown).

To determine whether inhibitory synaptic localization of IQSEC3 depends on the presence of gephyrin in cultured neurons, we knocked down endogenous gephyrin proteins at DIV8 and examined whether localization or stability of endogenous IQSEC3 protein was altered at DIV14 (Fig. 6). Notably, gephyrin KD with short hairpin RNA (shRNA) significantly decreased the number of endogenous IQSEC3 puncta, but not GAD67 puncta, suggesting that the maintenance of IQSEC3 at inhibitory synapses is dependent on gephyrin and that this interaction contributes to IQSEC3-dependent inhibitory synapse formation (Fig. 6; see Fig. 9, *F* and *G* for gephyrin KD characterization).
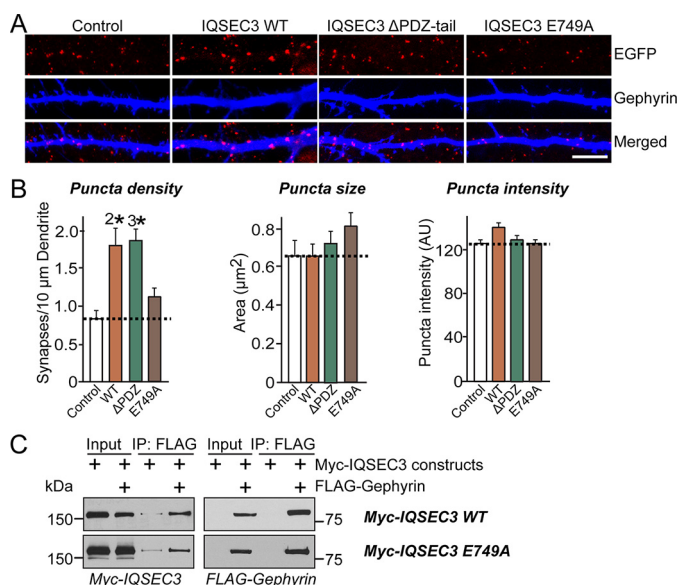
FIGURE 8. **IQSEC3 promotes inhibitory synapse formation that depends on its ARF-GEF activity but is independent of its PDZ-binding property.** *A,* representative images of cultured hippocampal neurons transfected at DIV10 with EGFP alone (*Control*) or together with the indicated IQSEC3 constructs. Neurons were analyzed by double immunofluorescence labeling for gephyrin (*red*) and EGFP (*blue*) at DIV14. *Scale bar,* 10 μm (applies to all images). *B,* summary graphs of the effect of overexpressing IQSEC3 constructs in neurons on gephyrin puncta density (*left*), gephyrin puncta size (*middle*), and gephyrin puncta intensity (*right*), measured using gephyrin as an inhibitory postsynaptic marker. At least five to eight dendrites per transfected neuron were analyzed and group-averaged. More than 500 gephyrin puncta were quantified in an individual image. Data are presented as means ± S.E. (^{2*}, $p < 0.01$; ^{3*}, $p < 0.001$ *versus* control group; Student's *t* test). *C,* co-immunoprecipitation experiment demonstrating that IQSEC3-E749A interacts with gephyrin. HEK293T cells were transfected with Myc-IQSEC3 or its indicated mutants alone or together with FLAG-gephyrin, and co-immunoprecipitation of gephyrin with IQSEC3 was assayed. A representative immunoblot visualized by ECL is shown. Input, 5%. *AU,* arbitrary units.

To corroborate this notion, we overexpressed a series of IQSEC3 deletion constructs with gephyrin binding activity or lacking gephyrin binding activity (Fig. 7). We found that overexpression of IQSEC3 aa 1–995 and IQSEC3 aa 336–1094 increased the number of gephyrin-positive synaptic puncta, whereas IQSEC3 aa 1–315 or IQSEC3 aa 336–995 did not (Fig. 7). To probe the reason for the failure of IQSEC3 aa 1–315 to increase gephyrin-positive synaptic puncta, we generated an additional set of IQSEC3 constructs that either lacked the ability to bind to PDZ-containing proteins (*e.g.* S-SCAM) or abolished its ARF-GEF activity (IQSEC3 E749A) (Fig. 8). We found that the IQSEC3 ΔPDZ C-tail (aa 1–1190), but not the dominant-negative E749A construct (while retaining the ability to interact with gephyrin; Fig. 8C), still boosted inhibitory synapse formation (Fig. 8). These results suggest that IQSEC3 promotes inhibitory synapse development through its Arf-GEF activity, not through its C-terminal PDZ-domain binding. In addition, our results support the conclusion that gephyrin-binding activity alone does not dictate the inhibitory synapse-promoting property of IQSEC3, because IQSEC3 aa 1–315 was able to bind well to gephyrin but lacked the SEC7 domain, which is critical for Arf-GEF activity.

Knockdown of IQSEC3 Decreases Gephyrin Puncta Size in Cultured Neurons—To address whether IQSEC3 is required for inhibitory synapse formation and function, we tested the effect of IQSEC3 KD using shRNAs targeting rat *Iqsec3*. Preliminary tests in HEK293T cells showed that, of the four designed shRNAs (B1–B4), only the B3 construct was effective, suppressing the level of co-expressed FLAG-IQSEC3 by ~80% (Fig. 9, *A* and *B*). The efficacy of the B3 construct against endogenous IQSEC3 was further confirmed in cultured rat cortical neurons infected with lentiviruses expressing B3 or control vector (control). Quantitative real time RT-PCR and semi-quantitative immunoblotting showed that B3 specifically decreased *Iqsec3* mRNA levels by ~70% (Fig. 9C) and protein levels by ~80%, without affecting gephyrin or PSD-95 protein levels (Fig. 9, *D* and *E*).

Next, to determine whether IQSEC3 KD alters synaptic morphology parameter, we transfected cultured neurons at DIV8 with lentiviral expression vectors for EGFP only (control) or EGFP together with *Iqsec3*-shRNA or *Iqsec3*-shRNA and shRNA-resistant full-length IQSEC3 expression vector (see Fig. 9H), and we immunostained transfected neurons at DIV14 for gephyrin. Surprisingly, in contrast to the robust effects of IQSEC3 gain-of-function (Fig. 5), IQSEC3 KD had no effect on gephyrin-positive inhibitory synapse numbers in dendrites or soma (Fig. 10, *A* and *B*). However, IQSEC3 KD significantly reduced gephyrin puncta size in dendrites and soma. Importantly, co-expression of an shRNA-resistant form of IQSEC3 (+rescue) completely abolished the deficits in gephyrin puncta size observed with IQSEC3 KD (Fig. 10, *A* and *B*), confirming that the observed phenotypes are not derived from off-target effects. Note that co-expression of the IQSEC3 rescue vector leads to IQSEC3 gain-of-function phenotypes (*i.e.* increased gephyrin puncta density). These results may appear to indicate that the expression level of the IQSEC3 rescue vector is too high to induce an IQSEC3-overexpression effect (data not shown). However, we rejected this interpretation because parallel experiments showed no increase in gephyrin puncta size (Fig. 10, *A* and *B*). Overall, our data are consistent with the idea that IQSEC3 is required for gephyrin clustering (Fig. 10, *A* and *B*).

Discussion

The presumption that inhibitory postsynaptic specialization is less elaborate than excitatory PSD has been increasingly challenged by rapid progress in our understanding of inhibitory synapse organization. Because inhibitory synapses are fundamentally different from excitatory synapses with regard to the nature of neurotransmitter receptors and associated proteins, the organizing principles underlying inhibitory synapse development are also likely different. Gephyrin is a key scaffolding molecule at inhibitory synapses, and its interaction with collybistin plays a major role in clustering of gephyrin and modulating $GABA_A$ receptor functions (4). Gephyrin also directly interacts with NL-2, which specifically drives postsynaptic assembly at perisomatic inhibitory synapses (9). However, in light of the molecular heterogeneity of inhibitory synapses, efficient inhibition requires that various inhibitory synaptic components, including gephyrin, are functionally and physically coupled. In this study, we identified a direct molecular interaction of gephyrin with IQSEC3, a previously unexplored inhibitory synaptic protein, and investigated its synaptic functions using various experimental approaches, including biochemistry, cell
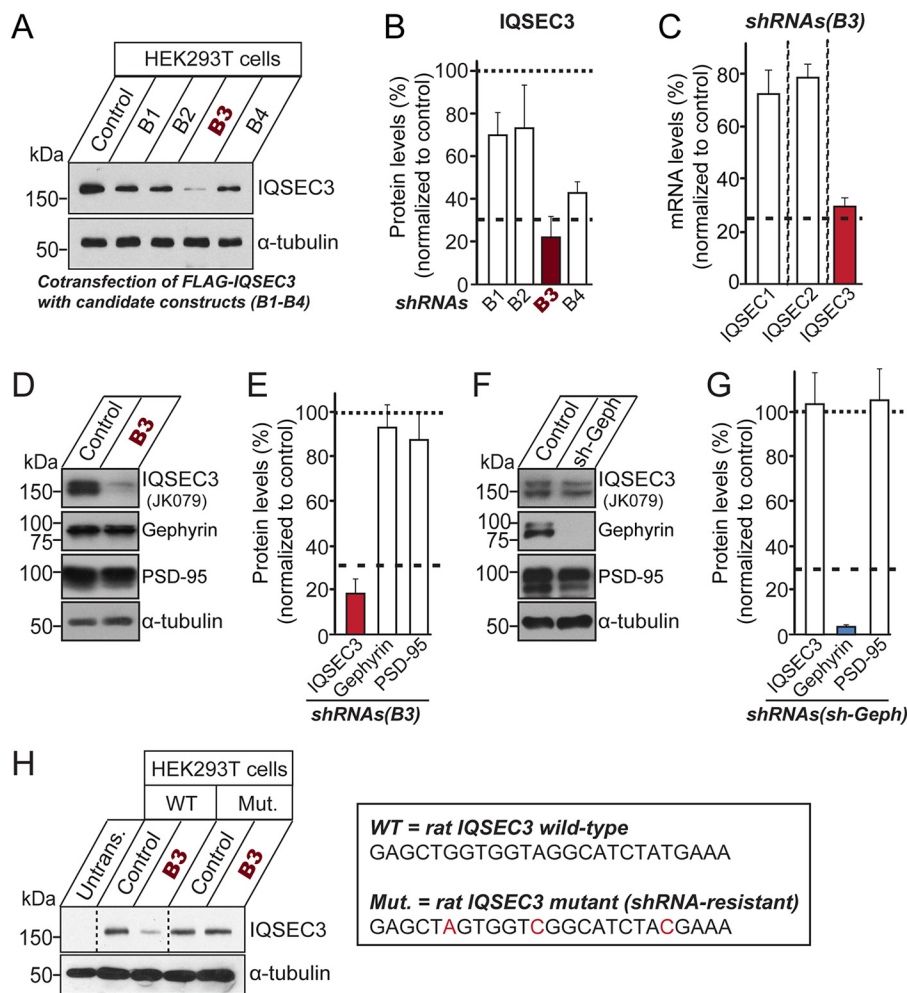
FIGURE 9. **Characterization of an *Iqsec3* shRNA construct in HEK293T cells and cultured neurons.** *A,* KD efficacies of shRNAs. Levels of IQSEC3 were measured by Western blotting in HEK293T cells co-transfected with FLAG-IQSEC3 and the indicated shRNA constructs. *B,* quantification of IQSEC3 levels from *A* normalized to control. Data are presented as means ± S.E. of three experiments. *C,* specificity of IQSEC3-KD construct, B3. Levels of mRNA (*Iqsec1–3*) were measured by quantitative RT-PCR in cultured cortical neurons infected at DIV3 with lentiviruses expressing *Iqsec3* shRNA (*B3*). mRNA was prepared at DIV10. Note that *Iqsec3* mRNA was specifically reduced. *D,* cultured cortical neurons were infected with lentiviruses expressing *Iqsec3* shRNA (B3) at DIV3 and subjected to immunoblotting with the indicated antibodies at DIV10. *E,* quantification of IQSEC3, gephyrin, and PSD-95 levels from *D* normalized to control. Data are presented as means ± S.E. of three experiments. *F,* cultured cortical neurons were infected with lentiviruses expressing gephyrin shRNA at DIV3 and subjected to immunoblotting with the indicated antibodies at DIV10. *G,* quantification of IQSEC3, gephyrin, and PSD-95 levels from *F,* normalized to control. Data are presented as means ± S.E. of three experiments. *H,* validation of the IQSEC3 shRNA-resistant construct. Levels of IQSEC3 were measured by Western blotting in HEK293T cells transfected with WT IQSEC3 or an IQSEC3 shRNA-resistant mutant construct (*Mut.*) alone or together with *Iqsec3* shRNA (B3). *Box at right* indicates the shRNA target sequences in WT *Iqsec3* and shRNA-resistant sequences in mutated *Iqsec3.*

biology, and knockdown-and-rescue. We made two principal findings as follows.

First, IQSEC3 is a new gephyrin-binding protein (Figs. 1, 3, and 4). The IQSEC family of Arf-GEF proteins is composed of three members, IQSEC1, IQSEC2, and IQSEC3, and both IQSEC2 and IQSEC3, but not IQSEC1, interact with gephyrin in heterologous cells. We mapped the binding sites in IQSEC3 to N- and C-terminal sites and in gephyrin to the G-domain. To the best of our knowledge, IQSEC3 is the first protein identified that binds to the G-domain of gephyrin; most other gephyrin-interacting proteins bind to either C- or E-domains. Therefore, it is tempting to speculate that IQSEC3 may regulate G-domain-mediated trimer formation by gephyrin (27). Indeed, knockdown of IQSEC3 markedly decreased gephyrin puncta size, an indicator of reduced clustering. In addition, our observation that gephyrin binds to two distinct sites in IQSEC3 suggests a possible U-shaped conformation of IQSEC3 when asso-

ciated with gephyrin, a result reminiscent of cytohesin 2 (another Arf-GEF), which exhibits a coiled-coil intramolecular interaction and shows full Arf-GEF activity only when in the open conformation (29).

Second, our gain- and loss-of-function experiments in cultured hippocampal neurons clearly establish the significance of IQSEC3 in inhibitory synapse development (Figs. 5 and 10). Overexpression of IQSEC3 strikingly increased inhibitory synapse density, whereas KD of IQSEC3 caused a decrease in gephyrin puncta size with no alternation in gephyrin puncta density. Intriguingly, we found that IQSEC3-mediated inhibitory synapse promotion is independent of PDZ protein binding, but instead it relies on its Arf-GEF activity (Fig. 8). It is also notable that overexpression of IQSEC3-E749A abolished the inhibitory synapse-promoting activity of IQSEC3, an effect that was not observed following IQSEC3 KD (Fig. 8). Incomplete KD of IQSEC3 protein expression cannot wholly account for this
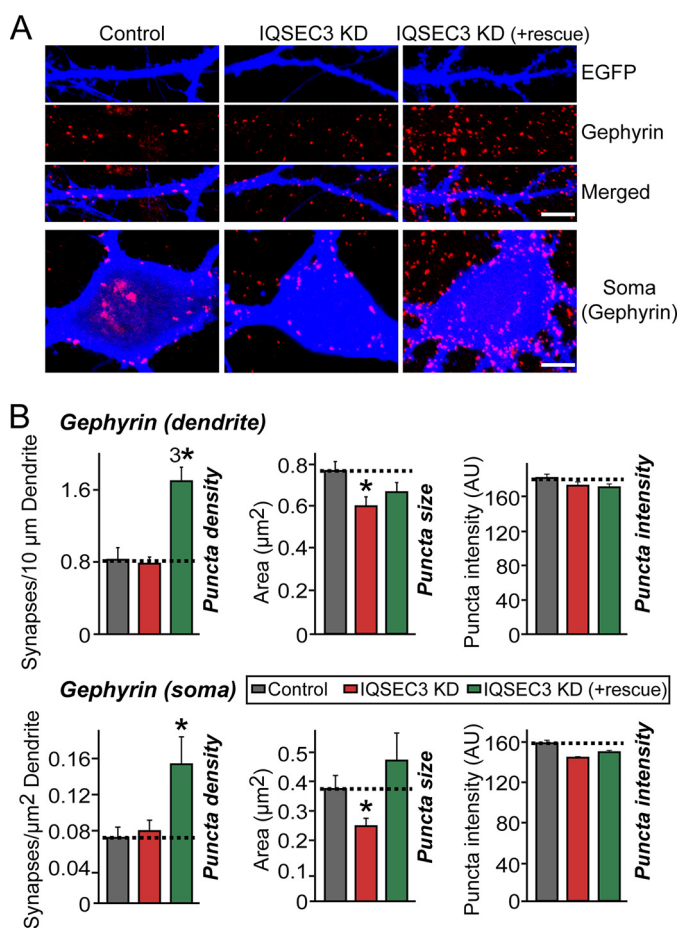
A

B

FIGURE 10. **IQSEC3 is required for maintenance of gephyrin clusters in cultured neurons.** *A*, representative images of both dendrites and soma of cultured hippocampal neurons transfected at DIV8 with lentiviral constructs expressing EGFP alone (*Control*), co-expressing EGFP with shRNAs against *Iqsec3* (*IQSEC3-KD*), or co-transfected with IQSEC3-KD and the shRNA-resistant IQSEC3 full-length vector (*+IQSEC3 rescue*). Neurons were analyzed by double immunofluorescence labeling for gephyrin (*red*) and EGFP (*blue*) at DIV14. *Scale bar*, 10 μm (applies to all images). *B*, summary graphs of the effects of IQSEC3 KD in neurons on gephyrin puncta density (*left*), gephyrin puncta size (*middle*), and gephyrin puncta intensity (*right*). At least five to eight dendrites or one soma per transfected neuron were analyzed and group-averaged. Data are presented as means ± S.E. (*, $p < 0.05$; [3]*, $p < 0.001$; ANOVA with Tukey's test). More than 850 gephyrin puncta were quantified in an individual image. *AU*, arbitrary units.

phenotypic discrepancy because IQSEC3 KD significantly reduced inhibitory synaptic transmission.[4] Instead, these data support the interpretation that the phenotype derived from IQSEC3-E749A substitution is a gain-of-function phenotype because it was not observed with IQSEC3 loss-of-function. Although further details remain to be determined, it is likely that residual IQSEC3 proteins remaining after KD are still functionally capable of activating Arf proteins that coordinate inhibitory synapse development. Regardless of the precise mechanisms, our data suggest that IQSEC3 employs diverse molecular mechanisms at inhibitory synapses and that Arf6 may also be involved in inhibitory synapse development. At excitatory synapses, IQSEC2, together with Arf6 signaling pathways, regulates synaptic activity-dependent removal of AMPA receptors (15). Moreover, Arf6 and its Arf-GEF, EFA6A,

coordinate excitatory synapse development (28), implying that actions of Arf6 signaling pathways operate in both excitatory and inhibitory synapses. Furthermore, it should be rigorously determined whether IQSEC3 acts as a GEF for specific Arf proteins and whether Arfs function in inhibitory synapse development together with IQSEC3.

In summary, our study illustrates the significance of the gephyrin-IQSEC3 complex in organizing inhibitory synapse development and provides compelling evidence to corroborate the idea that IQSEC3 is a critical factor in governing inhibitory synapse formation. The immediate goals of future studies should be to validate the postulated roles of IQSEC3 presented here using conditional KO and/or knock-in mice lacking gephyrin interactions to address whether IQSEC3 broadly mediates inhibition at specific synapse types in specific neuron types and by extension associated neural circuits.

Author Contributions—J. W. U., T. P., E. K., K. T., and J. K. conceived and designed the experiment. J. W. U., G. C., D. P., D. K., H. K., T. P., T. Y., and Y. L. performed the experiments. J. W. U., G. C., S. J., T. M., T. P., E. K., K. T., and J. K. analyzed the data. S. J. and J. K. contributed reagents, materials, and analysis tools. J. W. U. and J. K. wrote the paper.

References

1. Fritschy, J. M., Panzanelli, P., and Tyagarajan, S. K. (2012) Molecular and functional heterogeneity of GABAergic synapses. *Cell. Mol. Life Sci.* **69,** 2485–2499
2. Arancibia-Carcamo, I. L., and Moss, S. J. (2006) Molecular organization and assembly of the central inhibitory postsynapse. *Results Probl. Cell Differ.* **43,** 25–47
3. Papadopoulos, T., and Soykan, T. (2011) The role of collybistin in gephyrin clustering at inhibitory synapses: facts and open questions. *Front. Cell. Neurosci.* **5,** 11
4. Choii, G., and Ko, J. (2015) Gephyrin: a central GABAergic synapse organizer. *Exp. Mol. Med.* **47,** e158
5. West, A. E., and Greenberg, M. E. (2011) Neuronal activity-regulated gene transcription in synapse development and cognitive function. *Cold Spring Harb. Perspect. Biol.* **3,** a005744
6. Ko, J., Choii, G., and Um, J. W. (2015) The balancing act of GABAergic synapse organizers. *Trends Mol. Med.* **21,** 256–268
7. Tyagarajan, S. K., and Fritschy, J. M. (2014) Gephyrin: a master regulator of neuronal function? *Nat. Rev. Neurosci.* **15,** 141–156
8. Specht, C. G., Izeddin, I., Rodriguez, P. C., El Beheiry, M., Rostaing, P., Darzacq, X., Dahan, M., and Triller, A. (2013) Quantitative nanoscopy of inhibitory synapses: counting gephyrin molecules and receptor binding sites. *Neuron* **79,** 308–321
9. Poulopoulos, A., Aramuni, G., Meyer, G., Soykan, T., Hoon, M., Papadopoulos, T., Zhang, M., Paarmann, I., Fuchs, C., Harvey, K., Jedlicka, P., Schwarzacher, S. W., Betz, H., Harvey, R. J., Brose, N., *et al.* (2009) Neuroligin 2 drives postsynaptic assembly at perisomatic inhibitory synapses through gephyrin and collybistin. *Neuron* **63,** 628–642
10. Papadopoulos, T., Korte, M., Eulenburg, V., Kubota, H., Retiounskaia, M., Harvey, R. J., Harvey, K., O'Sullivan, G. A., Laube, B., Hülsmann, S., Geiger, J. R., and Betz, H. (2007) Impaired GABAergic transmission and altered hippocampal synaptic plasticity in collybistin-deficient mice. *EMBO J.* **26,** 3888–3899
11. Papadopoulos, T., Eulenburg, V., Reddy-Alla, S., Mansuy, I. M., Li, Y., and Betz, H. (2008) Collybistin is required for both the formation and main-

---

[4] J. W. Um and J. Ko, unpublished observations.

tenance of GABAergic postsynapses in the hippocampus. *Mol. Cell. Neurosci.* **39,** 161–169

12. Krueger, D. D., Tuffy, L. P., Papadopoulos, T., and Brose, N. (2012) The role of neurexins and neuroligins in the formation, maturation, and function of vertebrate synapses. *Curr. Opin. Neurobiol.* **22,** 412–422

13. Fukaya, M., Kamata, A., Hara, Y., Tamaki, H., Katsumata, O., Ito, N., Takeda, S., Hata, Y., Suzuki, T., Watanabe, M., Harvey, R. J., and Sakagami, H. (2011) SynArfGEF is a guanine nucleotide exchange factor for Arf6 and localizes preferentially at post-synaptic specializations of inhibitory synapses. *J. Neurochem.* **116,** 1122–1137

14. Sakagami, H., Katsumata, O., Hara, Y., Tamaki, H., Watanabe, M., Harvey, R. J., and Fukaya, M. (2013) Distinct synaptic localization patterns of brefeldin A-resistant guanine nucleotide exchange factors BRAG2 and BRAG3 in the mouse retina. *J. Comp. Neurol.* **521,** 860–876

15. Myers, K. R., Wang, G., Sheng, Y., Conger, K. K., Casanova, J. E., and Zhu, J. J. (2012) Arf6-GEF BRAG1 regulates JNK-mediated synaptic removal of GluA1-containing AMPA receptors: a new mechanism for nonsyndromic X-linked mental disorder. *J. Neurosci.* **32,** 11716–11726

16. Scholz, R., Berberich, S., Rathgeber, L., Kolleker, A., Köhr, G., and Kornau, H. C. (2010) AMPA receptor signaling through BRAG2 and Arf6 critical for long-term synaptic depression. *Neuron* **66,** 768–780

17. Morishige, M., Hashimoto, S., Ogawa, E., Toda, Y., Kotani, H., Hirose, M., Wei, S., Hashimoto, A., Yamada, A., Yano, H., Mazaki, Y., Kodama, H., Nio, Y., Manabe, T., Wada, H., *et al.* (2008) GEP100 links epidermal growth factor receptor signalling to Arf6 activation to induce breast cancer invasion. *Nat. Cell Biol.* **10,** 85–92

18. Tarpey, P. S., Smith, R., Pleasance, E., Whibley, A., Edkins, S., Hardy, C., O'Meara, S., Latimer, C., Dicks, E., Menzies, A., Stephens, P., Blow, M., Greenman, C., Xue, Y., Tyler-Smith, C., *et al.* (2009) A systematic, large-scale resequencing screen of X-chromosome coding exons in mental retardation. *Nat. Genet.* **41,** 535–543

19. Shoubridge, C., Tarpey, P. S., Abidi, F., Ramsden, S. L., Rujirabanjerd, S., Murphy, J. A., Boyle, J., Shaw, M., Gardner, A., Proos, A., Puusepp, H., Raymond, F. L., Schwartz, C. E., Stevenson, R. E., Turner, G., *et al.* (2010) Mutations in the guanine nucleotide exchange factor gene IQSEC2 cause nonsyndromic intellectual disability. *Nat. Genet.* **42,** 486–488

20. Ko, J., Kim, S., Valtschanoff, J. G., Shin, H., Lee, J. R., Sheng, M., Premont, R. T., Weinberg, R. J., and Kim, E. (2003) Interaction between liprin-α and GIT1 is required for AMPA receptor targeting. *J. Neurosci.* **23,** 1667–1677

21. Ko, J., Soler-Llavina, G. J., Fuccillo, M. V., Malenka, R. C., and Südhof, T. C. (2011) Neuroligins/LRRTMs prevent activity- and Ca^{2+}/calmodulin-dependent synapse elimination in cultured neurons. *J. Cell Biol.* **194,** 323–334

22. Kins, S., Betz, H., and Kirsch, J. (2000) Collybistin, a newly identified brain-specific GEF, induces submembrane clustering of gephyrin. *Nat. Neurosci.* **3,** 22–29

23. Mok, H., Shin, H., Kim, S., Lee, J. R., Yoon, J., and Kim, E. (2002) Association of the kinesin superfamily motor protein KIF1Bα with postsynaptic density-95 (PSD-95), synapse-associated protein-97, and synaptic scaffolding molecule PSD-95/discs large/zona occludens-1 proteins. *J. Neurosci.* **22,** 5253–5258

24. Woo, J., Kwon, S. K., Nam, J., Choi, S., Takahashi, H., Krueger, D., Park, J., Lee, Y., Bae, J. Y., Lee, D., Ko, J., Kim, H., Kim, M. H., Bae, Y. C., Chang, S., *et al.* (2013) The adhesion protein IgSF9b is coupled to neuroligin 2 via S-SCAM to promote inhibitory synapse development. *J. Cell Biol.* **201,** 929–944

25. Ko, J., Kim, S., Chung, H. S., Kim, K., Han, K., Kim, H., Jun, H., Kaang, B. K., and Kim, E. (2006) SALM synaptic cell adhesion-like molecules regulate the differentiation of excitatory synapses. *Neuron* **50,** 233–245

26. Gibson, J. R., Huber, K. M., and Südhof, T. C. (2009) Neuroligin-2 deletion selectively decreases inhibitory synaptic transmission originating from fast-spiking but not from somatostatin-positive interneurons. *J. Neurosci.* **29,** 13883–13897

27. Saiyed, T., Paarmann, I., Schmitt, B., Haeger, S., Sola, M., Schmalzing, G., Weissenhorn, W., and Betz, H. (2007) Molecular basis of gephyrin clustering at inhibitory synapses: role of G- and E-domain interactions. *J. Biol. Chem.* **282,** 5625–5632

28. Choi, S., Ko, J., Lee, J. R., Lee, H. W., Kim, K., Chung, H. S., Kim, H., and Kim, E. (2006) ARF6 and EFA6A regulate the development and maintenance of dendritic spines. *J. Neurosci.* **26,** 4811–4819

29. Hiester, K. G., and Santy, L. C. (2013) The cytohesin coiled-coil domain interacts with threonine 276 to control membrane association. *PLoS ONE* **8,** e82084